ELSEVIER

Biophysical Chemistry 58 (1996) 289–302

Biophysical Chemistry

Surface areas and packing constraints in POPC/$C_{12}EO_n$ membranes. A time-resolved fluorescence study

G. Lantzsch *, H. Binder, H. Heerklotz, M. Wendling, G. Klose

Universität Leipzig, Institut für Experimentelle Physik I, Linnéstrasse 5, 04103 Leipzig, Germany

Received 7 March 1995; revised 23 June 1995; accepted 26 June 1995

Abstract

The surface area occupied by nonionic detergents of the type $C_{12}EO_n$ ($n = 1–8$) in POPC/$C_{12}EO_n$ mixed membranes was studied by means of time-resolved resonance energy transfer (RET) between the fluorescent probe molecules NBD-PE and rhodamine-PE. The area data were interpreted within the frame of Israelachvili's concept of packing constraints yielding the critical packing parameter, f, as a measure of the asymmetry of the molecular shape of the membrane constituents. The asymmetry of the molecular shape of the detergent increases with the ethylene oxide chain length and correlates with the potency of the detergent to solubilize the bilayers and the reduction of the DPH order parameter. For $n = 1–3$, the membrane surface was found to expand by 0.25–0.30 nm^2 per incorporated $C_{12}EO_n$ molecule. This value corresponds to the cross section of one hydrocarbon chain in liquid–crystalline phases. On increasing n from $n = 4$ to $n = 8$ the net area per detergent molecule increases from 0.43 nm^2 to 1.16 nm^2. These surface requirements are consistent with a disordered, coiled conformation of the EO-chains hydrated with up to two water molecules per ethylene oxide unit. For $n > 5$ the limiting mole fraction of the bilayer saturation was deduced from the f-data in the two-component bilayer. DPH and NBD-PE fluorescence lifetime data are discussed to give an indication of the accessibility of the probe environment to water molecules.

Keywords: Detergents, non-ionic; Lipid bilayer; Resonance energy transfer; Fluorescence, time-resolved; Surface area; Critical packing parameter

1. Introduction

Oligo(ethylene oxide) acyl ethers (C_mEO_n) are composed of a hydrophilic EO-chain and an apolar acyl tail. The hydrophilic–hydrophobic balance of these molecules can be varied in a definite way by changing the number of CH_2- and/or EO-units. In an aqueous environment the ethylene oxides of the type C_mEO_n assemble into different aggregated structures depending on the number of methylene- and EO-units, i.e. m and n, as well as on the external conditions (temperature, water concentration) [1,2].

The amphiphilic nature of $C_{12}EO_n$ makes them very suitable to modify lipid membranes in order to study hydration forces [3–5] lyotropic [6,7] and thermotropic phase behaviour [8–10] and solubilization ([11–13], Heerklotz et al., in preparation). Regions

* Tel.: -341-9732474; fax: -341-9732497; e-mail: lantzsch@mp.physik.uni-leipzig.d400.de.

SSDI 0301-4622(95)00108-5

of lamellar as well as of micellar and hexagonal phases have been found in the ternary phase diagram of POPC/$C_{12}EO_n$-water with $n = 2$ and 4 thus indicating the capability of the detergent to induce the formation of nonlamellar aggregates. The formation of nonlamellar structures is closely related to solubilization of lipid membranes. The potency of the detergent to transform POPC/$C_{12}EO_n$ mixed vesicles into mixed micelles and thus to destabilize lamellar structures increases with the length of the EO-chain [12]. Otten et al. [10] used $C_{12}EO_8$ mixed with various saturated phosphatidylcholines to study the stages of the bilayer micelle transition. In a general context a detailed knowledge of the properties of detergent/lipid systems is important for several practical purposes such as reconstitution of functional membranes [14,15], isolation and purification of membrane proteins [16] and preparation of lipid vesicles by the detergent removal method [17,18].

The interactions between the surfactant molecules determine the geometry and stability of molecular aggregates. A simple but powerful method to correlate intermolecular forces with the structure of the aggregates is the concept of molecular packing constraints developed by Israelachvili et al. [19,20]. According to this concept the form of the aggregates can be deduced mainly from the forces acting between the amphiphiles. Recently, the usefulness of the concept of molecular packing constraints was demonstrated on lamellar hexagonal phase transitions of phosphatidylcholine/$C_{12}EO_8$ systems [9] as well as on the solubilization of lipid vesicles by $C_{12}EO_8$, which was interpreted in terms of the changing average shape of the component molecules [10].

Consequently, the determination of the structure of molecular assemblies and particularly of bilayers in combination with information about the molecular order and shape of its constituents is a prerequisite for the understanding of the phase behaviour and solubilization of lipid/detergent systems.

X-ray diffraction represents a well established method to investigate the geometry of lipid bilayers [21] as well as of $C_{12}EO_n$ lamellar systems [3,22,23] in terms of quantities as the thickness of the hydrophobic core or the surface area requirement of the molecules. Defect regions in multilamellar structures and separation of water can, however, distort the data [24,25]. Alternatively, ^{2}H-NMR spectroscopy was used to obtain respective structural information from deuterium order parameter profiles of the acyl chains [9,10,26–28]. Recently, Nagle [29] discussed that uncertainties are introduced mainly by the interpretation of the NMR data.

The efficiency of resonance energy transfer depends essentially on the distance between the energy donor and acceptor. The sensitivity range of this effect of usually 2–5 nm corresponds to the dimensions of a lipid bilayer in the normal direction thus offering a further possibility to study it's geometry. Usually, two fluorescent probes are associated with the bilayer as energy donor and acceptor. Fung and Stryer [30] considered the dependence of the transfer efficiency on the surface density of the acceptor and listed guidelines for the choice of the probe molecules. Davenport et al. [31] investigated the localization of fluorescent probes within phospholipid bilayers by means of RET. Recently, we demonstrated that time-resolved investigations for determining the surface area of the constituents in POPC/$C_{12}EO_n$ ($n = 2,4,6$) mixed membranes are advantageous compared with steady state measurements [32]. Because of its sensitivity fluorescence probe techniques are well suited for the investigation of dilute aqueous vesicle dispersions at a very high amount of excess water.

The main purpose of the present paper is to report about the geometry of POPC/$C_{12}EO_n$ membranes studied by means of time-resolved measurements of RET between fluorescent probes using a homologous series of the detergent. The results demonstrate that the surface area per molecule can be obtained by this technique. The analysis of fluorescence decay curves applied considers the relative position of the donor and acceptor fluorophores within the bilayer as well as the RET to both monolayers of the membrane. Fluorescent labeled lipids have been used as energy donor (NBD-PE) and acceptor (rhodamine-PE). The results are interpreted in terms of Israelachvili's concept of packing constraints and compared with solubilization data measured by means of isothermal titration calorimetry ([13], Heerklotz et al., in preparation). The systematic modification of the bilayer upon variation of the number of the ethylene oxide units between 1 and 8 allows to specify a qualitative different behaviour of detergents with 'longer' ($n >$

4) and 'shorter' EO-chains. Additional information about local molecular order has been extracted from the fluorescence anisotropy and lifetime of diphenylhexatriene and NBD-PE in order to complete the molecular picture of the mixed membrane.

2. Experimental

2.1. Materials and sample preparation

1-Palmitoyl-2-oleoyl-sn-glycero-3-phosphatidylcholine (POPC) and the fluorescent egg phosphatidyl-ethanolamine derivatives 7-nitrobenz-2-oxa-1,3 diazole-4-yl-PE and rhodamine-PE (NBD-PE and Rh-PE, respectively) were purchased from Avanti Polar Lipids (USA), the oligoethylenglycol-dodecylether ($C_{12}EO_n$; $n = 1-8$) from Nikko Chemicals Co. (Japan) and 1,6-diphenyl-1,3-hexatrien (DPH) from Serva (Germany). The substances were used without further purification.

Lipid vesicles were prepared as described previously [32]. The lipid, the detergent and the fluorophores, dissolved in methanol (spectroscopic grade) were mixed in definite relations, dried at room temperature and resuspended in water. The samples were rapidly vortexed two times for one minute each and stored overnight under nitrogen at 4°C. The diameter of the vesicles was characterized by means of QELS measurements to be about 100–400 nm (results not shown).

The concentration of POPC was adjusted to 500 μM. Usually two series of samples with detergent/lipid molar ratios $R = 0.33$ and 1 were prepared. The molar ratio Rh-PE/POPC, R_A, was varied between 0.001 and 0.02 at constant concentration of the donor NBD-PE (2.5 μM) to give a remarkable effect of RET. The acceptor concentration within the sample has been controlled by UV-VIS spectroscopy. In some preliminary experiments indications of a nonrandom distribution of the probe molecules within the bilayers were detected using molar ratios Rh-PE/POPC $R_A > 0.02$ or Rh- and NBD-dipalmitoylphosphatidylcholine instead of the respective egg yolk-PE derivatives. Therefore, these experimental conditions are excluded from the further work. DPH was used at molar ratio probe/lipid of 1/500. All samples were measured at room temperature (25°C).

2.2. Time-resolved fluorescence measurements

Time-resolved fluorescence measurements were performed on a modified LIF 200 spectrometer (ZWG Berlin) with nitrogen laser excitation at a wavelength of 337 nm.

The emission decays of DPH and NBD-PE were recorded at 430 nm and 520 nm, respectively, using a H-10 monochromator (Jobin-Yvon) with 8 nm slits.

Excitation and emission polarizers were used for RET and lifetime measurements in order to realize magic angle conditions. Experimental decay curves were analyzed by means of a non-linear iterative fitting algorithm including convolution of the excitation pulse with the delta pulse response function prescribed by Eq. 3 or by a sum of up to three exponentials. Usual test criteria were applied to check the quality of the fits.

Intensity-weighted average fluorescence lifetimes, τ_0, were calculated using

$$\tau_0 = \frac{\sum_{i=1}^{n} a_i \cdot \tau_i^2}{\sum_{i=1}^{n} a_i \cdot \tau_i} \qquad (1)$$

where a_i and τ_i are the preexponential factors and lifetimes, respectively.

We obtained time-resolved fluorescence anisotropy data from the intensity decays recorded with excitation and emission polarizers oriented parallel and perpendicularly. The analysis includes G-factor correction and the iterative fitting and deconvolution of sum and difference signals using exponential decay functions [33]. The orientational order parameter of DPH and NBD-PE was calculated according to [34,35]

$$S = \sqrt{\frac{r_\infty}{r_0}} \qquad (2)$$

where r_0 and r_∞ denote the limiting values of the time-resolved anisotropy at $t = 0$ and $t >> \tau_0$, respectively.

Steady state emission spectra were recorded on a Perking Elmer LS50 spectrometer.

2.3. Model of resonance energy transfer

The efficiency of RET depends essentially on the mean distance between energy donors and acceptors thus representing a useful tool to investigate the geometry of molecular aggregates by means of time-resolved fluorescence measurements. In lipid membranes we assume the donor and acceptor fluorophores to be submerged in definite depths and to be distributed randomly in the lateral plane. The radiationless deactivation of excited donors competes with the fluorescence emission giving rise to the fluorescence decay function [36]:

$$i(t) = i_0(t) \cdot N(t,d_1) \cdot N(t,d_2) \qquad (3)$$

$i_0(t)$ denotes the fluorescence decay of the donor in the absence of RET characterized by an average lifetime τ_0.

$N(t,d_1)$ and $N(t,d_2)$ are functions of the form [37,31]:

$$N(t,d_i) = \exp\left\{2\pi d_i^2 C_A \int_0^1 \times\left[1 - \exp\left(\left(-\frac{t}{\tau_0}\right)\left(\frac{R_0}{d_i}\right)^6 \beta^6\right)\right]\beta^{-3}d\beta\right\}$$

$$i = 1,2 \qquad (4)$$

describing the time dependence of RET between donors and acceptors distributed randomly on two parallel, infinite planes, which are separated by d_i, the distance of closest approach of donor–acceptor pairs. The two-dimensional acceptor concentration, C_A, is given in units of molecules per nm^2.

Note that integration of Eq. 4 yields an expression equivalent to Eq. 21 given in ref. [37]. The efficiency of RET changes very sharply at intermolecular distances around R_0, the critical Förster radius that usually amounts to 2–5 nm, a distance comparable to the thickness of lipid bilayers. Consequently, Eq. 3 considers the transfer of excitation energy within one side of the bilayer as well as the deactivation of donors induced by acceptors located within the opposite monolayer. Thus the interplane separations, d_1 and d_2, correspond to RET to both monolayers of the membrane as illustrated in Fig. 1.

The validity of the model used is limited to (i) low concentrations of donors and acceptors (low excitation limit and no excluded area effects), (ii) the absence of translational diffusion of the fluorophores on the time scale of the fluorescence lifetime of the donor and (iii) the absence of any time dependence of the critical Förster radius introduced possibly by the orientation factor implicit in R_0.

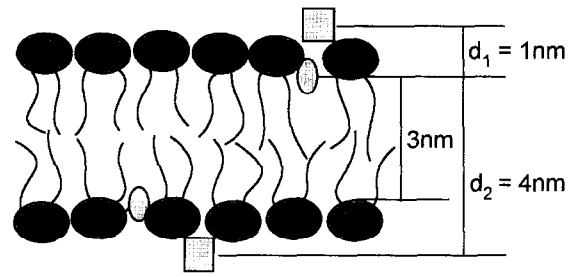

Fig. 1. Schematic representation of the layer model used to describe the resonance energy transfer in membranes. The donor (NBD) and acceptor (rhodamine) fluorophores covalently bound to PE are shown by open ellipses and squares, respectively.

3. Results and discussion

3.1. Fluorescence order parameters and lifetimes

DPH is buried between the hydrocarbon chains of the amphiphiles whereas the NBD-fluorophore was shown to probe the glycerol region of the bilayer [36,38].

In order to characterize the environment of the fluorescent probes incorporated into bilayers of pure POPC and of POPC/$C_{12}EO_n$ mixtures we measured fluorescence order parameters and emission lifetimes. The data are shown in Figs. 2 and 3 in dependence on the length of the ethylene oxide chain at two detergent/lipid molar ratios. A quite different behaviour of the two probe molecules was found.

On the one hand, no significant modifications of the NBD fluorescence order parameter could be detected (cf. Fig. 2A) indicating that the density of molecular packing around the lipid headgroups remains unaffected by the presence of EO moieties with up to 8 units. Also the lifetime of NBD-PE does not depend on n (cf. Fig. 3A). It shows, however, a systematic decrease with increasing R. The origin of this effect is not known. We note, that this dynamic quenching is not accompanied by changes of the

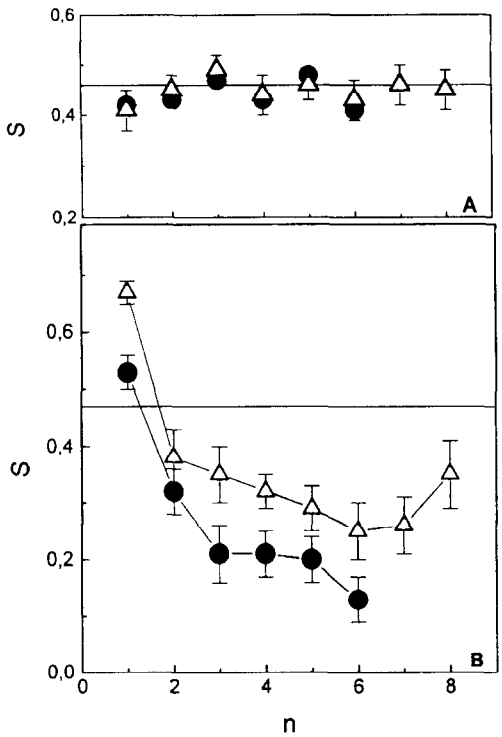

Fig. 2. Dependence of the fluorescence order parameter of (A) NBD-PE and (B) DPH in mixed POPC/$C_{12}EO_n$ membranes on the number of EO units at the detergent/lipid ratios, R, of (△) 0.33 and (●) 1. The error bars represent the standard deviation of 4...8 measurements per data point.

emission spectra. Mazères et al. found that the fluorescence quantum yield of the NBD group strongly depends on the polarity of the surrounding medium and also on the nature of the matrix [39].

On the other hand, the lifetimes and order parameters of DPH obviously change (cf. Fig. 3B, Fig. 2B). The continuous reduction of the order parameter, S, with the number of oxyethylene units, n, can be attributed to the increase of the surface area of the detergent (see below). Namely, lateral expansion should create additional free volume and thus a decreased packing density of the hydrocarbon chains. The small but significant relative increase of S for $n = 7$ and 8 is not yet understood. The average lifetime of DPH fluorescence is known to correlate with the DPH order parameter [33,40]. We found an analogous tendency of both quantities upon changes of the number of oxyethylene groups per detergent. Obviously the reduction of the density of molecular packing is accompanied by the dynamic quenching of DPH fluorescence. Possibly, this effect is caused by an increased probability of collisions between the fluorophore and water molecules [41]. The finding that addition of detergent to the lipid bilayer decreases the average order of the hydrocarbon chains as indicated by DPH order parameter agrees with the results of Thurmond et al. [9], who found that an increasing proportion of $C_{12}EO_8$ in phosphatidylcholine membranes leads to a significant reduction in magnitude of the S_{CD} order parameter profile.

The shorter acyl chain of the detergent induces a smaller average order of the hydrophobic core of the bilayers as expected. Contrary to the interrelation between S and τ_0 stated above the lower order parameter found with increasing molar ratio of the detergent predominantly correlates with a longer average DPH lifetime. In spite of the reduction of the molecular order the environment of the probe molecules is probably shielded from water by the

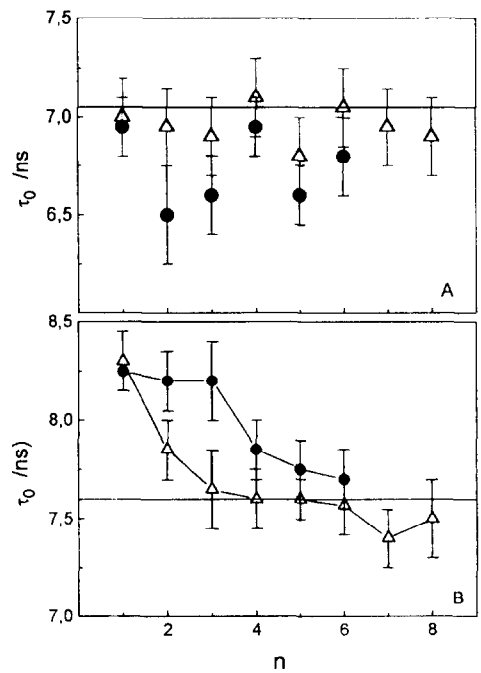

Fig. 3. Dependence of fluorescence lifetimes, τ_0, of (A) NBD-PE and (B) DPH in mixed POPC/$C_{12}EO_n$ membranes on the number of EO units, n, at the detergent/lipid ratios, R, of (△) 0.33 and (●) 1. The error bars represent the standard deviation of 2...4 measurements per data point.

presence of EO-chains in the bilayer. The EO moiety seems to compete locally with water associated with the lipid head group. This finding is consistent with the results of Zavoico et al. [42], who observed an increase of the DPH lifetime of about 1 ns in egg PC vesicles after the addition of unbranched alkanols. Most likely the hydroxyl groups replace water molecules within the hydrophilic membrane region. Varying the length of the alkanols the authors found a maximum of the DPH order parameter if the additive spans one monolayer. Under these circumstances probably no free volume was induced by the incorporation of the alkanol. In analogy we conclude that $C_{12}EO_1$ fits tightly between the POPC molecules thus giving rise to an enhancement of S relative to the pure lipid system (cf. Fig. 7).

3.2. Surface area of the detergent

Decay curves of NBD fluorescence measured in samples with increasing amounts of Rh-PE are shown in Fig. 4. The reduction of the average lifetime reflects the increased extent of energy transfer.

The application of the layer model requires at first the check of the restrictions listed in Section 2.3. Certainly, the limiting conditions of negligible lateral diffusion and of small concentrations of the fluorescent probes are realized in lipid membranes for donor lifetimes less than 10 ns and molar ratios of fluorescent probe/lipid used in this work [30,31]. However, the validity of the third condition (iii), i.e. the neglection of any time dependence of the extent of RET on the relative orientations between the donors and acceptors is not obvious. Therefore, it must be justified by inspection of the temporal as well as the spatial and angular ranges of averaging the orientational factor, κ^2, contributing to R_0.

The analysis of the time-resolved fluorescence anisotropy curves of NBD-PE in $POPC/C_{12}EO_n$ membranes yields a mean correlation time of molecular reorientations of 2.1 ± 0.3 ns. Assuming a similar value for reorientations of the acceptor and relating these correlation times to the average lifetime of donor fluorescence, $\tau_0 = 6.8 \pm 0.3$ ns, we notice that the limit of fast reorientational averaging appears to be met satisfactorily. Furthermore, the averaging of

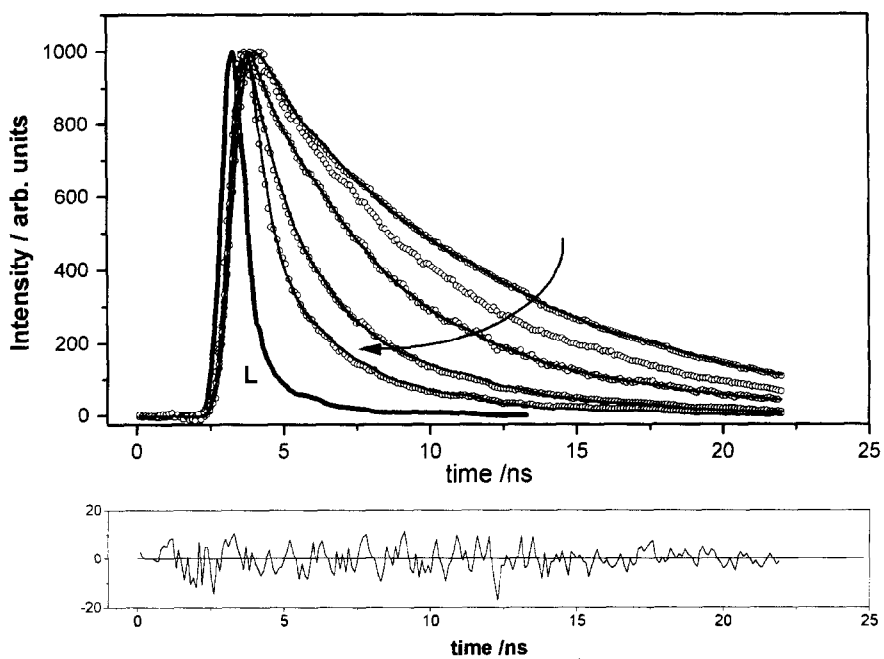

Fig. 4. NBD-PE (donor) fluorescence decays (○) in $POPC/C_{12}EO_2$ membranes in the presence of rhodamine-PE (acceptor) at molar acceptor/lipid ratios of $R_A \cdot 10^2 = 0.24$, 0.56, 1.12 and 1.68. L denotes the laser response. The curves (solid lines) are calculated according to Eq. 3. The residuals corresponding to the decay measured at $R_A = 0.56$ are shown at the bottom in order to give a typical example of the quality of the fits.

κ^2 should consider the restricted angular range of reorientations accessible to the fluorophores during the lifetime of the excited state. Using the concept of axial depolarization factors applied to lipid membranes [31] it is shown in the appendix that decay functions of the form given by Eq. 3 represent a good approximation for the system investigated.

Thus the time-resolved fluorescence data are analyzed in terms of the layer model mentioned above in order to determine the surface area of the detergent molecule in the membrane. In the fitting procedure the lipid concentration C_A was assumed to be the only free adjustable parameter in the function given by Eq. 3.

The lifetime τ_0 of NBD-PE in membranes without acceptor was measured separately. The Förster radius of $R_0 = 4.6$ nm was calculated previously [32] according to

$$R_0 = 9.768 \cdot 10^3 \left(\kappa^2 Q_D n^{-4} J_{DA}\right)^{1/6} \quad (5)$$

using $n = 1{,}4$, $\kappa^2 = 2/3$, $Q_D = 0.27$ and $J_{DA} = 2.4\ 10^{-13}$ cm^{-6} mol^{-1} for the refractive index of the medium, the dipole–dipole orientation factor, the quantum yield of the donor in the samples without acceptors and the overlap integral, respectively.

The distances between the donor and acceptor planes, d_1 and d_2, were derived from the bilayer geometry [3] and from the penetration depths of the fluorophoric groups. In PC-membranes the rhodamine and NBD fluorophores were found to be located near the lipid–water interface [32] and within the glycerol region [36,38], respectively. No changes of the fluorescence spectra of the NBD and rhodamine derivatives have been observed after addition of any $C_{12}EO_n$ used in this work. Therefore, we conclude the localization of the fluorophores to remain unchanged within the modified membranes. Assuming a thickness of the hydrophobic core and of the headgroup region of 3 nm and of 0.6 nm, respectively, we used $d_1 = 1$ nm and $d_2 = 4$ nm. This choice takes into account an average projection of the acceptor fluorophore from the membrane interface (see Fig. 1) the magnitude of which was estimated from the chemical structure of rhodamine in analogy to Davenport et al. [31]. The projection of the dipole responsible for the energy-transfer-accepting properties is about 0.25–0.65 nm, giving the mean distance from the membrane surface of 0.4 ± 0.1 nm.

A non-linear algorithm was used to fit the decay curves by optimization of the acceptor concentration, C_A, at constant d_1 and d_2, yielding acceptable fits (cf. residual plot Fig. 4). Alternatively we treated d_1 and/or d_2 as free adjustable parameters, additionally to C_A.

However, no significant improvement of the sum of squared residuals was obtained. These attempts yielded very unstable results in most cases with confidence intervals of the d-values typically larger than 1 nm. Apparently, the subtle modifications of the calculated decays induced by changes of the distance parameters are below the noise level of the experimental signals and, consequently, cannot be resolved. Therefore, the fitting algorithm was restricted to C_A only using the prescribed values for d_1 and d_2 given above.

Making use of the relation $C_A = R_A/A$ the average lateral area per lipid, A, was calculated by linear regression of C_A versus R_A, the molar ratio acceptor/lipid present in the samples. Assuming additivity of the areas of the components [43], A is given by

$$A = A_L + R \cdot A_D \quad (6)$$

where R is the molar ratio detergent/lipid. The net area of one lipid molecule, $A_L = 0.65$ nm^2, was taken from pure POPC bilayer data [3,32]. After rearrangement of Eq. 6, the net area per detergent, A_D, is

$$A_D = \frac{A - A_L}{R}. \quad (7)$$

Fig. 5 shows the A_D data drawn in dependence on the length of the EO-chain at two different detergent/lipid molar ratios. The areas of the detergents with up to three EO units are about 0.25–0.30 nm^2. This value corresponds approximately to the cross section of a hydrocarbon chain in liquid–crystalline phases. For $n > 3$ the area of the detergent increases continuously with n, the number of EO-groups per molecule, up to 1.16 nm^2 for $C_{12}EO_8$. Rösch et al. [44] estimated the cross section of extended EO-chains in the all trans and helical conformations. The respective values of 0.19 nm^2 and 0.28 nm^2 are significantly smaller than the measured ones and

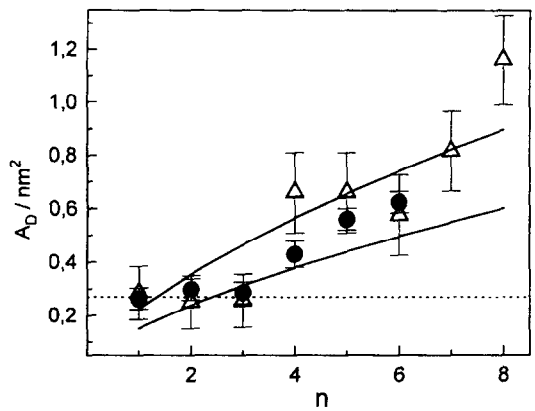

Fig. 5. Surface area occupied by one $C_{12}EO_n$ molecule, A_D, for $n = 1$–8 in POPC bilayers at molar detergent/lipid molar ratios R of (△) 0.33 and (●) 1. The lines represent the cross section of spheres the volume of which was calculated by using the molecular weight of n EO units and a density ρ of 1 g cm^{-3}. The upper line considers additionally the volume of two water molecules per EO unit. The horizontal dotted line corresponds roughly to the cross section of one hydrocarbon chain in the liquid-crystalline bilayer. The limits of experimental errors are estimated from the standard deviation of the slope of the linear regressions of 5–6 C_A values versus R_A as well as from repeated measurements of the same data points.

should, furthermore, not depend on the length of the ethylene oxide chain.

In order to imagine the area requirement of a completely disordered EO-chain in the membrane plane we estimated the cross section of a sphere the volume of which was calculated using the molecular weight of n ethylene oxide units and a density of 1 g/cm^3. Additionally, the hydration was taken into account by inclusion of the volume of two water molecules per EO-unit [45,46]. The A_D data of the detergents with $n \geqslant 2$ fit between the two curves calculated from this simple geometrical consideration thus indicating a disordered, coiled conformation of the EO chain to be more likely than an extended one. No differences of A_D between the samples with $R = 1$ and $R = 0.33$ could be detected within the limits of experimental error.

The A_D values have been determined assuming a constant membrane thickness and the additivity of lipid and detergent surface areas. Both assumptions seem to be critical because the incorporation of detergent into the bilayer gives rise to the fluidization of the lipid causing in this way a reduction of the thickness of the hydrophobic core of the bilayer coupled with the increase of the surface area per lipid [47]. Lateral expansion on the one hand and contraction in the normal direction on the other have opposite consequences on the average distance between donors and acceptors and therefore are expected to compensate each other at least partially. Indeed, the efficiency of energy transfer between NBD-PE and Rh-PE in POPC vesicles was shown to be independent on temperature thus confirming this hypothesis experimentally [32]. Therefore we neglect possible consequences of the detergent induced fluidization on the geometry of the bilayer.

However, the shorter acyl chain of the detergent is expected to reduce the average thickness of the mixed membranes in comparison with the pure lipid bilayer. The thickness of the hydrophobic core in fully hydrated bilayers of $C_{12}EO_3$, $C_{12}EO_4$ and $C_{12}EO_6$ was 1.91 nm, 1.65 nm and 1.36 nm, respectively, as determined by means of X-ray scattering [23]. König [3] measured the thickness of POPC/$C_{12}EO_n$ bilayers. At a molar ratio $R = 0.5$ the respective quantity decreases from 3.8 nm for $n = 2$ down to 3.55 nm for $n = 8$. Extrapolation to the higher molar ratio $R = 1$ yields a reduction of the membrane thickness by 0.5 nm for $n = 8$ relative to the POPC bilayer (3.8 nm). Assuming for a rough estimate that this reduction is related exclusively to the hydrophobic core, actually, a smaller distance parameter $d_2 < 4$ nm should be used to fit the fluorescence decays.

However, the precise thickness of the hydrophobic core is still unknown in the systems investigated and therefore an arbitrary variation of the parameter d_2 will introduce an additional degree of uncertainty into the data treatment. Instead, we consistently used a constant thickness parameter $d_2 = 4$ nm to fit the decay data of the different lipid/detergent mixtures as noted before.

In order to estimate the effect of the variation of d_2 on the area data we calculated theoretical decay curves corresponding to the reduced membrane thickness given above for $n = 8$. In a first step we generated decay data with $d_2 = 3.5$ nm and $A = 0.78$ nm^2. We assumed the area to be correlated with d_2 by the condition of incompressibility, i.e. a constant volume of the hydrophobic core: $(d_2 - d_1) \cdot A = 0.65$ nm$^2 \cdot 3$ nm $= 0.78$ nm$^2 \cdot 2.5$ nm $=$ const. Fitting of

Table 1
Area per surfactant molecule, A_D, and critical packing parameter, f, as determined by RET

System	Area per detergent molecule (nm^2)				Packing parameter f
	RET	X-ray			
		[3]	[22]	[23]	
POPC	0.65 ± 0.03 [a]	0.66 ± 0.02			0.65
$C_{12}EO_1$	0.26 ± 0.03 [b]				
$C_{12}EO_2$	0.27 ± 0.03 [b]	0.26 ± 0.02			
$C_{12}EO_3$	0.29 ± 0.03 [b]		0.368		0.72
$C_{12}EO_4$	0.43 ± 0.03 [b]	0.40 ± 0.02	0.426	0.43 ± 0.02	0.50
$C_{12}EO_5$	0.55 ± 0.03 [b]			0.45 ± 0.02	0.39
$C_{12}EO_6$	0.62 ± 0.04 [b]		0.516	0.48 ± 0.02	0.34
$C_{12}EO_7$	0.81 ± 0.12 [c]			0.54 ± 0.03	0.26
$C_{12}EO_8$	1.16 ± 0.12 [c]	0.60 ± 0.02			0.18

X-ray diffraction data of A_D, taken from the literature, are shown for comparison.
[a] From ref. [32].
[b] Values refer to $R = 1$.
[c] Values refer to $R = 0.33$.

the theoretical decay curve by means of our standard algorithm with the incorrect value $d_2 = 4$ nm yields an apparent molecular area of 0.71 nm^2, i.e. a value about 10% smaller than the input area. We conclude that if d_2 is actually smaller than 4 nm, our analysis would underestimate the membrane area.

Taking into account a realistic range of d_2 our rough estimate shows that the data drawn in Fig. 5 and listed in Table 1 represent the lower limit of the lateral areas of the detergent in the membrane with a systematic error not exceeding 10%.

Surface areas of some $C_{12}EO_n$ in pure detergent [23,24] and mixed POPC/detergent systems [3] are known from previous X-ray diffraction measurements. We found good agreement with our data for $n = 2$ and $n = 4$ (cf. Table 1). At $n > 4$ the areas obtained by the RET method systematically exceed the respective X-ray data to an increasing degree. About the possible reasons for this discrepancy we can only speculate at present.

On the one hand, if we assume that the longer EO-chains increase the thickness of the headgroup region than the efficiency of energy transfer will be reduced and, consequently, our analysis would result in a smaller area of the detergent. For the thickness of the hydrophilic part of the bilayer we originally used 0.6 nm, a value that is about 4 nm smaller than the Förster radius, R_0. The increase of the corresponding distance parameter d_1 from 1 nm up to an unrealistic value of nearly $R_0/2$ has, however, no measurable effect on the amount of RET within one monolayer of the membrane. Moreover, it appears not unlikely that some units of the EO-chains are dived into the hydrocarbon moiety [12,48] and therefore any assumption concerning the variation of the thickness of the interfacial layer would be vague.

On the other hand, we emphasize the quite different preparation techniques of samples for fluorescence and X-ray diffraction measurement's giving either a dilute aqueous vesicle suspension or a relatively viscous dispersion with lipid concentrations differing by more than three orders of magnitude.

Molecular areas of $C_{12}EO_n$ are also obtained by means of various monolayer techniques [49–52]. Most of the data for pure detergent systems with $n < 7$ exceed the respective areas given in Table 1 slightly. Naumann et al. published area requirements of the detergent in DPPC/$C_{12}EO_n$ mixtures at least two times greater than the data given by the other authors. We believe, however, that a direct comparison of molecular areas in monolayer and bilayer systems is problematic and therefore we exclude the monolayer data from the discussion.

Furthermore, the considerable discrepancies between the area requirements of the detergent obtained by means of RET and X-ray diffraction for $n = 7$, 8, stated above, should be weakened if one takes into account the limited precision of our data

due to the absence of measurements at the higher molar ratio ($R = 1$) of the detergent in the mixtures. We emphasize that the relative error is inversely proportional to R (cf. Eq. 7). The analysis in terms of the layer model is restricted to the lamellar phase, i.e. mixed vesicles. In order to avoid solubilization of the lamellae the composition of the samples is limited to R smaller than the critical molar ratio of membrane saturation R_{sat} (see below). In the case of $C_{12}EO_8$ and $C_{12}EO_7$ the R_{sat} values of 0.54 and 0.75, respectively ([12], Heerklotz et al., in preparation, [53]), are found just above the molar ratio used and therefore the choice of a higher R in order to increase the precision of the A_D data is impossible. It should be reminded that the mixed micelles formed at $R > R_{sat}$ do not correspond to the applied model and therefore their presence would falsify the area data.

3.3. Molecular asymmetry and membrane stability

Israelachvili et al. [19,20] introduced the critical packing parameter of an amphophil in order to quantify its molecular shape:

$$f = v/l_c \cdot a_0 \qquad (8)$$

where a_0 is the optimum area per molecule at the hydrophobic–hydrophilic interface. v is the molecular volume of the hydrophobic moiety of the amphophil formed by one or two hydrocarbon chains. The critical chain length, l_c, sets a limit for the maximum extended length of the hydrocarbon chains in the aggregate.

Amphiphils with $f < 1/3$ are likely to form spherical micelles [19,20]. Nonspherical micelles, bilayers and inverted structures are expected if $1/2 > f > 1/3$, $1 > f > 1/2$ and $f > 1$ [20], respectively. Consequently, the shape of the aggregate can be predicted from the geometry of its constituents.

In order to calculate the critical packing parameter of the systems investigated we used the empirical formulae given by Tanford [54]:

$$l_c \approx (0.15 + 0.1265 \cdot n_h)\, nm$$

$$v \approx k \cdot (27.4 + 26.9 \cdot n_h) \cdot 10^{-3}. \qquad (9)$$

That means, we approximate the critical length by the length of an extended saturated acyl chain containing n_h methylene groups. v and l_c were calculated with $n_h = 11$ and $n_h = 17$ for the detergent ($k = 1$) and lipid ($k = 2$) respectively. k is the number of hydrocarbon chains per amphophil. No correction was done for the double bond of the oleic acid chain of POPC because its influence was estimated to be less than 2% of the length given by Eq. 9. We calculated the critical packing parameter, f, of POPC and $C_{12}EO_n$ from Eqs. 8 and 9 equating the molecular areas determined by the RET method (cf. Table 1) with the optimum area, a_0.

The f-values of POPC, $C_{12}EO_3$ and $C_{12}EO_4$ are within the boundaries typical for lamellar phases (cf. Table 1 and Fig. 6). Indeed, these three amphiphils were found to form lamellar phases over a wide concentration range at room temperature [1]. The pure detergents with $n = 5$, 6, 7 and 8 are known to form micelles in an aqueous environment at room temperature [1,55–57]. The packing parameters, f, estimated for these detergents on the basis of our measurements decrease from 0.39 to 0.15, thus reflecting the preference of these amphiphils to assemble into micelles correctly.

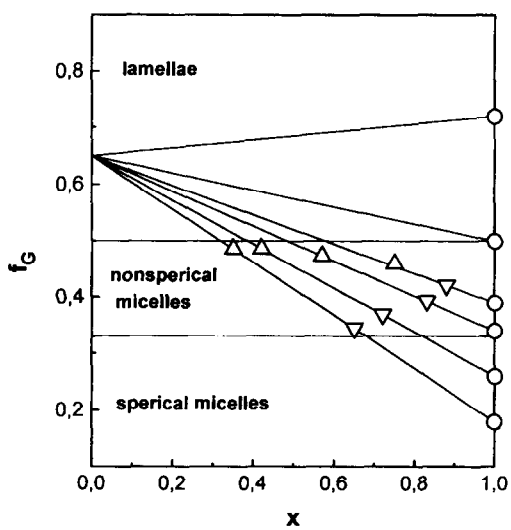

Fig. 6. Dependence of the critical packing parameter, f_G, calculated by means of Eq. 8 versus the mole fraction of the detergent, x, in POPC/$C_{12}EO_n$ mixtures. The symbols denote the mole fraction of bilayer saturation, x_{sat} (△) and solubilization, x_{sol} (▽), both taken from ref. [12]. The critical packing parameters of the pure detergents are shown by circles at $x = 1$.

A mixture of POPC with $C_{12}EO_n$ ($n = 5$–8) shows a transition between lamellar and micellar phases upon increasing mole fraction of the detergent, x. This transition is characterized by the coexistence of bilayers and micelles in the concentration range $x_{SAT} < x < x_{SOL}$ according to the model of solubilization proposed by Lichtenberg [58]. The bilayers present at low x are saturated with detergent if its composition reaches x_{SAT} and consequently, the formation of mixed micelles starts. In the coexistence range the composition of bilayers and micelles is given by x_{SAT} and x_{SOL}, respectively, independent on the overall mole fraction x in the sample. Solubilization completes at $x = x_{SOL}$, i.e. at higher mole fractions of the detergent only micelles exist.

Within the frame of the concept of molecular packing constraints the critical mole fractions x_{SAT} and x_{SOL} should correspond to definite values of the critical packing parameter that characterize the limits of bilayer and micelle stability, respectively. We calculated the effective packing parameter in $POPC/C_{12}EO_n$ mixtures, f_G, as the weighted average of the packing parameters of the lipid and detergent, f_L and f_D, respectively, e.g.

$$f_G = x \cdot f_D + (1 - x) \cdot f_L \quad (10)$$

Obviously, f_G changes as a linear function of x between the pure component values f_L and f_D as shown in Fig. 6. For $n = 5$ to 8 these straight lines intersect the limit of bilayer stability, $f = 0.5$, shown by a horizontal line. The respective mole fractions at $f = 0.5$ are in good agreement with the critical mole fractions x_{SAT} of the $POPC/C_{12}EO_n$ binary systems determined experimentally ([13], Heerklotz et al., in preparation, [53]).

In Fig. 6 the limiting compositions of the mixed micelles, x_{SOL}, indicate the upper boundaries of the coexistence regions established experimentally for $n = 5$–8 ([13], Heerklotz et al., in preparation). The corresponding packing parameters decrease from 0.41 ($n = 5$) to 0.34 ($n = 8$) and thus are found in the range typical for nonspherical micelles. For $n = 7$ and 8 the increase of the amount of detergent in the mixed micelles will reduce the critical packing parameter below the lower limit of stability of nonspherical micelles at $f = 0.33$. Consequently we expect a change of the micellar shape leading ultimately to spherical aggregates, which are really found in $C_{12}EO_8$ aqueous dispersions [55]. On the other hand the less asymmetric molecules $C_{12}EO_5$ and $C_{12}EO_6$ form nonspherical micelles in an aqueous environment [55–57].

According to the concept of opposing forces [54] the optimal surface area of an amphophil is determined by the competition of attractive and repulsive forces acting in the interfacial region. The surface area of $C_{12}EO_n$ with $n > 2$ was found to increase with the length of the ethylene oxide chain. Furthermore it exceeds the expected cross section of a dodecyl chain in liquid crystalline bilayers of about 0.25 nm^2. We conclude therefore that the changes of the A_D values are controlled mainly by the repulsive forces originating from the head groups, i.e. the ethylene oxide chains. That means that the cross section of the EO-chain determines the surface requirement per detergent molecule. Therefore we identified the area per headgroup, a_0, with A_D, the lateral area determined by means of RET method, as outlined before.

However, for $C_{12}EO_n$ with $n < 3$ we found A_D values of about 0.25 nm^2 corresponding to the cross section of an acyl chain in the liquid crystalline state. We conclude that in these cases the repulsion between the hydrocarbon tails controls the A_D data and therefore they cannot be interpreted as the area of the hydrophilic part of the amphophil, which could be smaller.

Consequently, the detergents with the shorter EO-chains can be characterized possibly by an inversely asymmetrical molecular shape that, however, cannot be quantified in more detail. Inverse micellar and hexagonal phases are really found in aqueous $C_{12}EO_2$ and $C_{12}EO_2/POPC$-systems [1,6] even at a high degree of hydration.

4. Summary and conclusions

Fluorescence resonance energy transfer yields information about the geometry of bilayers formed in surfactant aqueous dispersions. The sensitivity range of this method is determined in a decisive way by the Förster radius of the donor acceptor pair chosen. In our case the R_0 extends beyond the bilayer thickness. Consequently, the model of fluorescence deac-

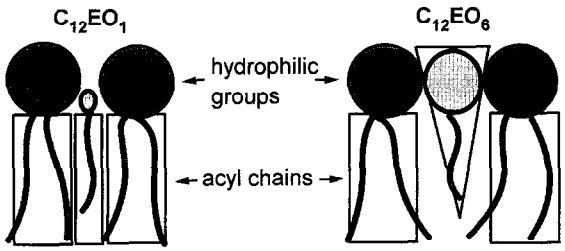

Fig. 7. Schematic depiction of the insertion behaviour of a molecule $C_{12}EO_n$ with $n = 1$ (left) and $n = 6$ (right) into POPC membranes.

tivation includes RET to acceptors located in both layers of the membrane. The analysis applied allows to determine the surface area of the lamellae. Assuming additivity of the surface requirements of the components we found that the area per detergent in POPC/$C_{12}EO_n$ membranes increases with the number of EO-units per detergent. Within the framework of Israelachvili's concept of molecular packing constraints this area increase is expressed in terms of the critical packing parameter, f, giving a measure of the asymmetry of molecular shape.

Detergent molecules with more than three EO-units, i.e. $n > 3$, are characterized by a more asymmetrical shape than the lipid. Therefore they are found to destabilize the POPC bilayer as indicated by the decreased DPH order parameter as well as by the tendency to solubilize the membranes for $n > 4$. On the other hand the $C_{12}EO_n$ with the shorter EO-chains ($n < 3$) are assumed to fit into the bilayer without a marked disturbing effect. Even a moderate decrease of the 'fluidity' of the hydrocarbon core was observed after addition of $C_{12}EO_1$ to the POPC vesicles. The incorporation of $C_{12}EO_n$ with shorter and longer EO-chains into a lipid membrane is illustrated schematically in Fig. 7.

The effective molecular shape in the POPC/$C_{12}EO_n$ mixtures changes with the mole fraction of the detergent. For $n > 4$ the limiting mole fraction of bilayer saturation was deduced from the f data in the two-component bilayer. These data agree well with respective values determined previously ([13], Heerklotz et al., in preparation) thus confirming the limit of bilayer stability usually adapted to $f = 0.5$. The potency of $C_{12}EO_n$ to destabilize the bilayer increases with the ethylene oxide chain length and consequently it correlates with the asymmetry of the molecular shape of the detergent.

Acknowledgements

This work was supported by the Deutsche Forschungsgemeinschaft (SFB 294).

Appendix A

The dynamic average of the orientation factor of RET between a donor and an acceptor fluorophore located on two parallel planes is given by [31]:

$$\kappa^2(\beta) = (1 - 3\beta^2)^2 S_D S_A + \frac{1}{3}(1 - S_D) + \frac{1}{3}(1 - S_A) + \beta^2[S_D(1 - S_A) + S_A(1 - S_D)]$$

$$\beta = \frac{d_i}{r} \qquad (11)$$

where d_i and r denote the distance between the planes and fluorophores, respectively. S_D and S_A are order parameters characterizing the range of orientations accessible to the emission dipole of the donor and the absorption dipole of the acceptor, respectively. Within the frame of the layer model Eq. 4 modifies by substitution of $R_0^6 \cdot 3/2 \cdot \kappa^2(\beta)$ for R_0^6

$$N(t,d_i) = \exp\left\{2\pi d_i^2 C_A \int_0^1 \left[1 - \exp\left(\left(-\frac{t}{\tau_0}\right)\left(\frac{R_0}{d_i}\right)^6 \frac{3}{2}\kappa^2(\beta)\beta^6\right)\right]\beta^3\right\}$$

$$i = 1,2. \qquad (12)$$

Decay curves calculated according to Eq. 12 for various interplane distances and order parameters are shown in Fig. 8A. The special case $S_A = S_D = 0$ is equivalent to the dynamic random average of $\kappa^2 = 2/3$ described by Eq. 4. The respective decays deviate clearly from the dependencies obtained for completely ordered fluorophores, i.e. $S_A = S_D = 1$. For

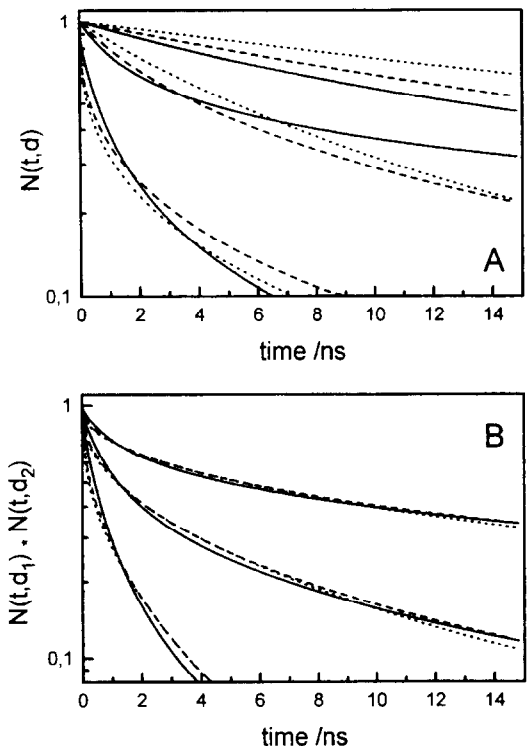

Fig. 8. Decay curves (A) $N(t,d)$ and (B) $N(t,d_1)\cdot N(t,d_2)$ calculated according to Eq. 12 for order parameters (————) $S_D = S_A = 1$, (– – –) $S_D = S_A = 0.5$ and (· · ·) $S_D = S_A = 0$. In (A) the interplane distance was $d = 1$ nm, 4 nm and 6 nm for the lower, central and upper set of curves, respectively. The acceptor concentration, C_A, corresponds to a molar acceptor/lipid ratio of $R_A = 0.02$ and an area per lipid of $A_L = 0.65$ nm^2. In (B) the decays are calculated for interplane distances $d_1 = 1$ nm and $d_2 = 4$ nm. C_A corresponds to $R_A = 0.02$, 0.01 and 0.005 for the lower, central and upper set of curves, respectively.

the small interplane distance ($d = 1$ nm) typical for RET within one monolayer the orientation of the fluorophores induces a slower or steeper decay at short and longer times, respectively. For RET across the hydrophobic core of the bilayer, i.e. $d = 4$ nm, $N(t,d)$ decreases more slowly at longer times (> 4 ns) in comparison with the case of randomly oriented fluorophores.

Intermediate order parameters ($S_A = S_D = 0.5$) reduce these deviations from the random case partially. If one takes the mean fluorescence order parameter of NBD-PE in POPC/$C_{12}E_n$ membranes ($S = 0.47 \pm 0.05$) as a good approximation to the order parameters of the respective transition dipoles, the curves with $S_A = S_D = 0.5$ correspond roughly to the membrane system investigated.

This analysis proofs that the restricted reorientations of the fluorophores should be considered generally, i.e. Eq. 4 represents a poor approximation to the more general decay law given by Eq. 12 at least for order parameters $S > 0.5$. However, the energy transfer in bilayers is described typically by a product of two functions $N(t,d_1)\cdot N(t,d_2)$ (cf. Eq. 3). The combination of interplane distances ($d_1 = 1$ nm, $d_2 = 4$ nm) of the fluorophores used leads to a partial ($S_A = S_D = 1$) or almost complete ($S_A = S_D = 0.5$) compensation of positive and negative deviations from the decay calculated from the random average of κ^2 (see Fig. 8B). Note that the most pronounced changes of the decays are caused by the acceptor concentration, C_A, representing the parameter within the focus of interest. Small deviations between the isotropic case and the curve calculated with $S_A = S_D = 0.5$ become obvious at a longer time ($t > \tau_0$). However, the curves are rescaled to a steeper decay with increasing C_A, thus reducing the effect of this inaccuracy because of the low fluorescence intensity really present at longer times. Therefore we conclude that Eqs. 3 and 4 can be used as a good approximation to analyze the fluorescence decays in the systems investigated.

References

[1] D.J. Mitchell, G.J.T. Tiddy, L. Waring, T. Bostock and M.P. McDonald, J. Chem. Soc. Faraday Trans. I, 79 (1983) 975.
[2] M.J. Schick and M. Decker, Nonionic Surfactants, Phys. Chem. Surf. Sci. Series, New York, 1987.
[3] B. König, Ph.D. thesis, University Leipzig (1992).
[4] F. Volke, St. Eisenblätter and G. Klose, Biophys. J., 67 (1994) 1882.
[5] St. Eisenblätter, J. Galle and F. Volke, Chem. Phys. Lett., 228 (1994) 89.
[6] S.S. Funari and G. Klose, Chem. Phys. Lipids, 75 (1995) 145.
[7] G. Klose, St. Eisenblätter and B. König, J. Coll. Interf. Sci. (1995) (in press).
[8] B. Mädler, G. Klose, A. Möps, W. Richter and C. Tschierske, Chem. Phys. Lipids, 71 (1994) 1.
[9] R.L. Thurmond, D. Otten, M.F. Brown and K. Beyer, J. Phys. Chem., 98 (1994) 972.
[10] D. Otten, L. Löbbecke and K. Beyer, Biophys. J., 68 (1995) 584.

[11] H. Heerklotz, H. Binder and G. Lantzsch, J. Fluoresc., 4/4 (1994) 349.
[12] H. Heerklotz, H. Binder, G. Lantzsch and G. Klose, Biochim. Biophys. Acta, 1196 (1994) 114.
[13] H. Heerklotz, G. Lantzsch, H. Binder, G. Klose and A. Blume, Chem. Phys. Lett., 235 (1995) 517.
[14] M. Ollivon, O. Eidelman, R. Blumenthal and A. Walter, Biochemistry, 27 (1988) 1695.
[15] J.-L. Rigaud, M.-T. Paternostre and A. Bluzat, Biochemistry, 27 (1988) 2677.
[16] D.A. Haugen and M.J. Coon, J. Biol. Chem., 251 (1976) 7929.
[17] T.M. Allen, A.Y. Romans, H. Kercret and J.P. Segrest, Biochim. Biophys. Acta, 601 (1980) 328.
[18] O. Zumbuehl and H.-G. Weder, Biochim. Biophys. Acta, 640 (1981) 252.
[19] J.N. Israelachvili, Intermolecular and Surface Forces, Academic Press, San Diego, 1985.
[20] J.N. Israelachvili, D.J. Mitchell and B.W. Ninham, J. Chem. Soc. Faraday Trans. II, 9 (1976) 1525.
[21] A. Tardieu, V. Luzzati and F.C. Reman, J. Mol. Biol., 75 (1973) 711.
[22] A. Carvell, D.C. Hall, I.G. Lyle and G.J.T. Tiddy, Faraday Discuss. Chem. Soc., 81 (1986) 223.
[23] G. Klose, St. Eisenblätter, J. Galle and U. Dietrich, Langmuir (1994) (submitted).
[24] M. Klèman, C.W. Williams, M.J. Costello and T. Gulik-Krzywicki, Philosoph. Mag., 35 (1977) 33.
[25] K. Gawrisch, W. Richter, A. Möps, P. Balgavy, K. Arnold and G. Klose, Studia Biophys., 108 (1985) 5.
[26] H. Schindler and J. Seelig, Biochemistry, 14 (1975) 2283.
[27] R.J. Pace and S.I. Chan, J. Chem. Phys., 76 (1982) 4217.
[28] R.L. Thurmond, S.W. Dodd and M.F. Brown, Biophys. J., 59 (1991) 108.
[29] J.F. Nagle, Biophys. J., 64 (1993) 1476.
[30] B.K.-K. Fung and L. Stryer, Biochemistry, 17 (1978) 5241.
[31] L. Davenport, R.E. Dale, R.H. Bisby and R.B. Cundall, Biochemistry, 24 (1985) 4097.
[32] G. Lantzsch, H. Binder and H. Heerklotz, J. Fluoresc., 4/4 (1994) 339.
[33] H. Binder, G. Lantzsch and K. Dittes, Wiss. Z. Karl-Marx-Univ., Math.-Naturwiss. Reihe, 38, 6 (1989) 569.
[34] G. Lipari and A. Szabo, Biophys. J., 30 (1980) 489.
[35] F. Jähnig, Proc. Natl. Acad. Sci., 76 (1979) 6361.
[36] G. Lantzsch, Ph.D. thesis, University Leipzig (1989).
[37] P.K. Wolber and B.S. Hudson, Biophys. J., 28 (1979) 197.
[38] A. Chattopadhyay and E. London, Biochemistry, 26 (1987) 39.
[39] S. Mazères, V. Schram, S. Fery-Forgues, J.F. Tocanne and A. Lopez, Biophys. J., 68 (1995) A303.
[40] C.D. Stubbs, T. Koyama, K. Kinosita and A. Ikegami, Biochemistry, 20 (1981) 4257.
[41] C. Ho and C.D. Stubbs, Biophys. J., 63 (1992) 897.
[42] G.B. Zavoico, L. Chandler and H. Kutchai, Biochim. Biophys. Acta, 812 (1985) 299.
[43] G. Klose, S. Brückner, V. Yu. Bezzabotnov, S. Gordelly and Yu.M. Ostanevich, Chem. Phys. Lipids, 41 (1986) 293.
[44] M. Rösch, Tenside, 9 (1972) 23.
[45] A. Zulauf, K. Weckström, J.B. Hayter, V. Degiorgio, M. Corti, J. Phys. Chem., 89 (1985) 3411.
[46] E.M. Lee, R.K. Thomas, P.G. Cummins, E.J. Stables, J. Penfold and A.R. Rennie, Chem. Phys. Lett., 162(3) (1989) 196.
[47] G. Cevc and D. Marsh, Phospholipid Bilayers: Physical Principles and Models, Wiley, New York, 1987.
[48] V.A. Volkov, Kolloid. Z. (Moscow) 36 (1974) 941.
[49] M.J. Rosen and D.S. Murphy, Langmuir, 7 (1991) 2630.
[50] M.J. Rosen, A.W. Cohen, M. Dahanayake and X.Y. Hua, J. Phys. Chem., 86 (1982) 541.
[51] J.H. Clint, Surfactant Aggregation, Blackie, Glasgow, 1992.
[52] C. Naumann, C. Dietrich, J.R. Lu, R.K. Thomas, A.R. Rennie, J. Penfold and T.M. Bayerl, Langmuir, 10 (1994) 1919.
[53] K. Edwards and M. Almgren, J. Colloid Interf. Sci., 147 (1991) 1.
[54] C. Tanford, The Hydrophobic Effect, Wiley and Sons, New York, 1973.
[55] P.-G. Nilsson, H. Wennerström and B. Lindman, J. Phys. Chem., 87 (1983) 1377.
[56] D.J. Cebula and R.H. Ottewill, Colloid Polym. Sci., 260 (1982) 1118.
[57] R. Zana and C. Weil, J. Phys. Lett., 46 (1985) 953.
[58] D. Lichtenberg, R.J. Robson and E.A. Dennis, Biochim. Biophys. Acta, 737 (1983) 285.